Contents lists available at Science-Gate

International Journal of Advanced and Applied Sciences

Journal homepage: http://www.science-gate.com/IJAAS.html

Multi-effect evaporator desalination powered by geo-solar thermal energy

Ibrahim Alenezi *

Department of Chemical Engineering and Material Science, Faculty of Engineering, Northern Border University, Arar, Saudi Arabia

ARTICLE INFO

Article history:
Received 7 February 2021
Received in revised form
30 April 2021
Accepted 19 May 2021

Keywords:
Geo-solar desalination
Multi-effect
Solar pond
Renewable energy

ABSTRACT

The abundance of solar energy in Saudi Arabia makes it the most promising option for use in water desalination. A salinity gradient solar pond (SGSP) is one of the most encouraging direct solar heat collectors. Increasing the gradient zone depth of the SGSP to 0.6m allows it to sustain the low operating temperature of single-or multi-effect evaporators (MEE) for 9 months of the year. The unique innovation of utilizing the heat of deep well water to support the operation of a system with such a low operating temperature provides feed water at up to 55°C, which means only 11.2kJ of heat energy is required to heat each 1kg of water to the MEE's evaporation temperature. This is 9.7% of the energy required when using surface seawater. A MATLAB simulation tool was developed to model the coupling of an SGSP with an MEE and was validated with experimental data collected for the climatic conditions of Saudi Arabia. It is well known that a conventional thermal desalination plant is cost-intensive, but the coupling model study of SGSP–MEE shows its operational feasibility at much lower costs.

1. Introduction

Saudi Arabia and the surrounding arid Middle East countries rely heavily on well-water and seawater to provide usable water for drinking, irrigation, and industrial purposes. Water should not be used directly for most of these purposes without being treated or desalinated and these arid states depend significantly on thermal desalination to produce potable water. However, conventional thermal desalination is energy-intensive and not a preferable option due to the cost of construction, operation, and maintenance, in addition to environmental pollution issues (Sharif et al., 2011). It has been estimated that producing 22–25 million cubic meters of water from desalination daily would require 204–230 million tonnes of oil per day (Kalogirou, 2001). According to an estimate by the governmental water authority in Saudi Arabia in 2017, each cubic meter of water could cost the government almost $10 using these conventional desalination plants (Porteous, 1983).

At the same time, the solar potential is considerably high in Saudi Arabia, with average annual direct normal irradiation exceeding 2000kWh/m^2 everywhere in the country, and daily direct normal irradiation as high as 7300Wh/m^2 in the northwest of the country, where the skies are clearest (Zell et al., 2015). According to data from NASA for 2020, the average annual all-sky horizontal insolation in Tabuk city in north-western Saudi Arabia is 6211Wh/m^2-day, 103% higher than in London, UK, where it is 3047Wh/m^2-day. The irradiation in Tabuk being double that in London is reflected in their respective temperatures, since the average annual temperature for each day in Tabuk is 21.5°C while it is recorded at 10.8°C in London, UK (NASA, 2021).

Solar energy technologies can be classified into two main types based on the way of utilizing the energy: Direct and indirect solar radiation collectors. The flat plate collector (FPC) is an example of an indirect solar device, while the salinity gradient solar pond (SGSP) is one of the solar collectors that directly converts the solar beam into heat.

In Madve Lake, Transylvania, in 1902, Kalecsinsky first reported a temperature gradient due to water salinity. This salinity gradient arose naturally due to heat inside the Madve Lake and gradually increased until the temperature reached 80ºC (Dickinson and Cheremisinoff, 1980; Kreider and Kreith, 1981) This observation encouraged researchers to construct an SGSP. In 1964 Tabor

* Corresponding Author.
Email Address: i.alenezi@nbu.edu.sa
https://doi.org/10.21833/ijaas.2021.08.009
Corresponding author's ORCID profile:
https://orcid.org/0000-0001-5169-3028

constructed similar non-convecting solar ponds in several countries including Israel, India, Kuwait, Italy, and Australia. Two of these ponds suffered destruction due to reaching boiling temperature (Lu et al., 2001; Hull et al., 1989).

Based on mathematical models developed by Duffie and Beckman (2006), a salinity gradient is a unique and simple system that collects sunlight and stores heat for long periods. A typical SGS pond consists of three layers (Fig. 1). The top layer, the upper convecting zone, is about 0.3m deep, which allows sunlight to penetrate and prevents the middle layer from evaporating. In the UCZ the temperature is very close to the ambient temperature. Next, the non-convecting zone (NCZ) is the middle layer, where both salinity and temperature increase with depth, which prevents convection even at high temperatures. The bottom layer is the lower convecting zone (LCZ), which has the highest temperature and salinity. The collected heat is stored in this region and can either be exchanged inside the pond or delivered outside the SGSP. The thickness of the LCZ is responsible for heat storage and temperature variation. As the thickness increases, the heat storage capacity increases and the temperature tends to be more stable.

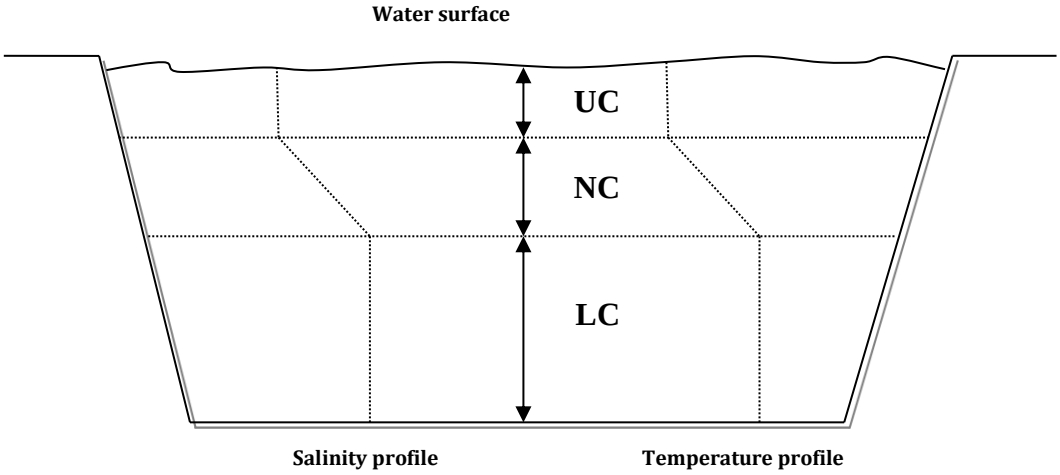

Fig. 1: Salinity and temperature profiles through the salinity gradient solar pond zones

Mesa et al. (1997) stated that 70 % of all seawater distillation is produced by using multi-stage flash distillation (MSF) and multiple-effect distillation (MED) (Mesa et al., 1997; Duffie and Beckman, 2006). Micale et al. (2009) reported that MED has approximately 12.5% market share. Both MED and MSF are energy-intensive, which means they are not cost-effective, making the use of abundant solar energy for the thermal desalination process attractive (Micale et al., 2009). Garman and Muntasser (2008) reviewed the parameters of a MED plant coupled with an SGSP. They showed that the total number of effects determines the capacity of the desalination plant. They analyzed the performance of a 4-effect plant and found that the amount of thermal energy needed is proportional to the surface area of the solar pond. Moreover, they determined the optimal thicknesses of the upper convecting zone (UCZ), non-convecting zone (NCZ), and lower convecting zone (LCZ) to be 0.3m, 1.1m, and 4m respectively, to sustain the best performance. They also determined that under optimal conditions, the plant could produce 6000m^3 of distilled water per day (Garman and Muntasser, 2008). Ophir and Lokiec (2005) performed several experiments in Israel to investigate the economic feasibility of multi-effect evaporators (MEE) and evaluated which desalination process was most cost-effective. They observed that low-temperature MEEs operate at ~70ºC and result in the most efficient operation. The authors concluded that the energy demand and the use of competitive building materials make MED the most economical distillation plant. The report by Ophir and Lokiec (2005) found that an MEE plant with five effects can produce distilled water at a rate of \$0.45/m^3 and each of the five effects can potentially produce 20,000m^3 per day (Ophir and Lociek, 2005).

A comparison study was conducted by Ophir and Lokiec (2005) to determine the most efficient and economically viable process available. They compared MED and MSF plants of the same capacity (100,000m^3 per day). To ensure identical levels of daily distilled water production, a five-effect MED plant and a two-stage MSF plant were observed. The authors reported that the capital expenditure (CAPEX) of the MEE plant was 10.5% lower than that of MSF. Furthermore, the MED plant had a lower operating expenditure (OPEX) due to lower chemical, labor, and electricity consumption. For example, an MSF plant consumed \$0.175/m^3 in electricity costs while the MEE required just \$0.06/m^3 (Ophir and Lociek, 2005).

Shahzad et al. (2018) examined the efficacy of a MED system operated using thermocline energy from the sea, which produced a nearly twofold improvement in desalination efficiency over the previous methods, attaining about 18.8% of the ideal thermodynamic limit for desalination. The effectiveness of a porous medium in a solar pond was investigated by Hongsheng et al. (2020), who

achieved an increase of 6°C in the maximum pond temperature using this method.

So far, the highest number of effects that have been used is 55, in the plant at Al Ain in the United Arab Emirates. Even this plant is designed to produce only 500m^3 daily (0.13 MGPD). Newer, well-engineered MED plants can work at the lower temperature of 60°C, though it has been reported that the Eilat plant in Israel and the Trapani plant in Italy have been working successfully at 55ºC since 1992. Many other plants in the United Arab Emirates, such as Mirfa, Jebel Dhanna, and Sila, are designed to generate desalination at a top brine temperature (TBT) of 58.5ºC (Al-Shammiri, 1999). This is because areas that receive high levels of solar radiation, without vegetation cover and with dry soils, provide effective thermal insulation of water underground.

Guo et al. (2020) investigated the performance improvement of MED salination systems achieved by preheating seawater. They achieved a gained output ratio (GOR) of 0.46%–9.26% with four preheaters and up to 22.65% with ten preheaters.

Building on the observation about thermal insulation underground, the present study investigated the use of well water instead of seawater as feedwater and showed that the greater the depth of the well, the higher the measured water temperature. Therefore, in many wells whose depth is about one kilometer, the water temperature at this depth should be maintained at about 50–55°C, and this does not vary greatly between summer and winter unless the water is exposed to cold conditions during its transport through the pipeline to the desalination plant.

2. Process modeling

The literature on modeling of MEE is sparse and that on coupled MEE–SGSP is even more limited. The forward-feed configuration of a multiple-effect evaporation system is not widely used for desalination.

This paper presents a new model for coupling the multiple-effect evaporation process (MEE) with the salinity gradient solar pond, using both the heat from solar energy and deep-well water as a source of heated water.

The model of MEE evaporators offered by Geankoplis (1993) and El-Dessouky and Ettouney (2002) has been adapted to meet the requirements of this study. In addition to the solar pond hot water, the system includes a series of evaporators, a pre-heater, and a mechanical vapor compressor, as illustrated in Fig. 2. The number of evaporators is initially set to 4, and mass and heat balance were used to create MATLAB code to solve this model using an iterative approach. The system is rated to produce 1kg/s of distilled water with the assistance of mechanical vapor compression.

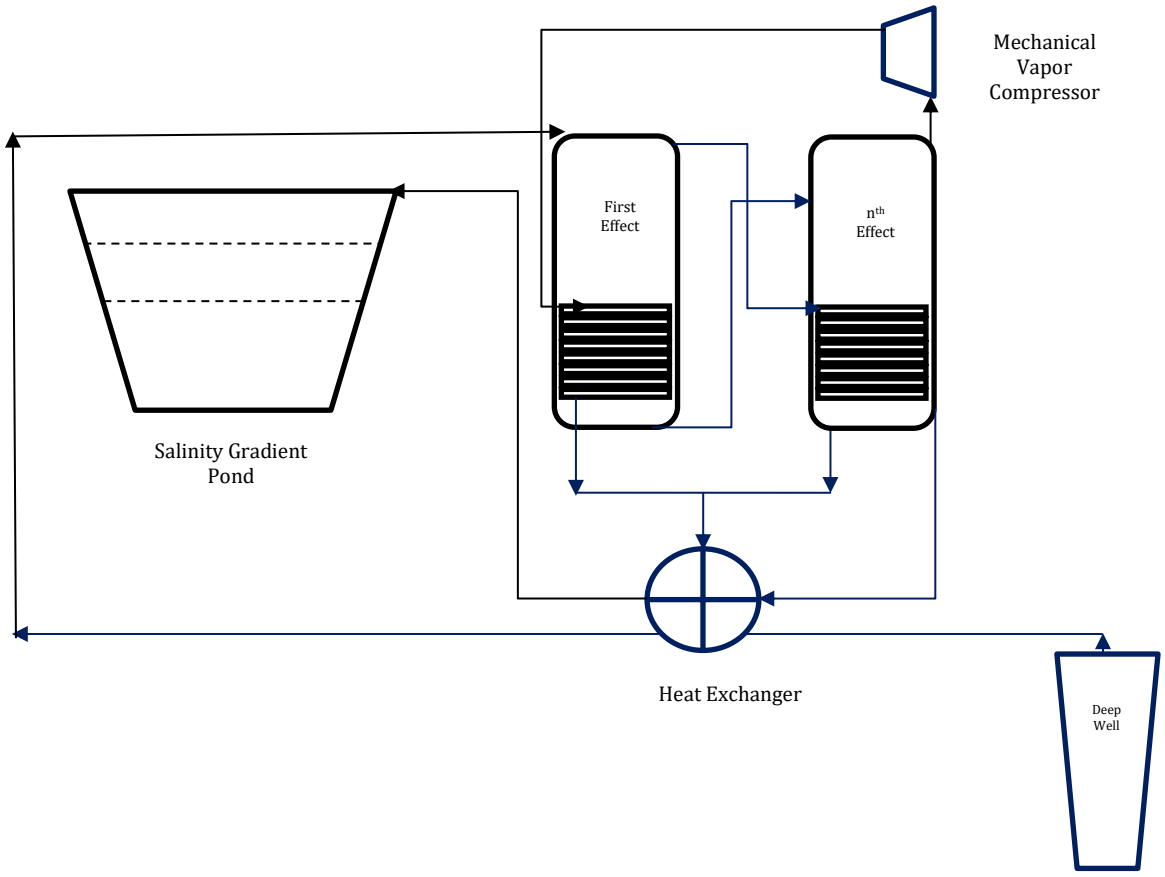

Fig. 2: Geo-solar desalination system

In the forward-feed configuration, the direction of heat, brine, and vapor flow is from left to right, i.e., from effect 1 to effect *n*.

In general, based on the principle of conservation of energy, the stored energy is equal to the rate of heat entering the storage zone minus the rate of heat loss. Hence, the steady-state correlation function for the storage zone is:

$$\rho_s C_{ps} A x_s \frac{dT_s}{dt} = Q_{srs} - Q_{st} - Q_{sb} - Q_{sw} - Q_{se} \quad (1)$$

The salinity pond model is validated with a real solar pond performance in Kuwait (Sharif et al., 2011). The solar irradiation calculation is validated with both measured field data in three different locations in the Middle East and with NASA data in the year 2020 irradiation data (Sharif et al., 2011).

The salty water can be treated as a binary mixture of fresh water and salt. Therefore, the feed flow rate (F) is the sum of the distilled flow rate (D) and the brine flow rate (B). For the first effect, this can be expressed as:

$$F = D_1 + B_1 \quad (2)$$

The concentration balance for the first effect can be obtained from:

$$X_f F = X_b B_1 \quad (3)$$

and for the other effects:

$$X_i B_i = X_{(i-1)} B_{(i-1)} \text{ for } i > 1 \quad (4)$$

The total distillate water is simply the summation of each effect product ($D = \sum_{i=1}^{n} D_i$). The thermal load, Q_i, is given by:

$$Q_1 = S\lambda_s \text{ and } Q_i = D_i\lambda_i \text{ for } i > 1 \quad (5)$$

The required thermal load is assumed to be constant, i.e., $Q_i = Q_j$ for all i, j. In each effect ($i > 1$), the thermal load can be considered as the previous effect's thermal heat carried by the vapor. Therefore, the equation is:

$$D_i = \frac{D_1\lambda_1}{\lambda_i} \quad (6)$$

The brine flow rate from the first effect can be estimated simply from Eq. 2 ($B_1 = F - D_1$) and the brine flow rates of the other of the evaporators:

$$B_i = B_{(i-1)} - D_i \quad (7)$$

The calculated latent heat is shown in Fig. 3.

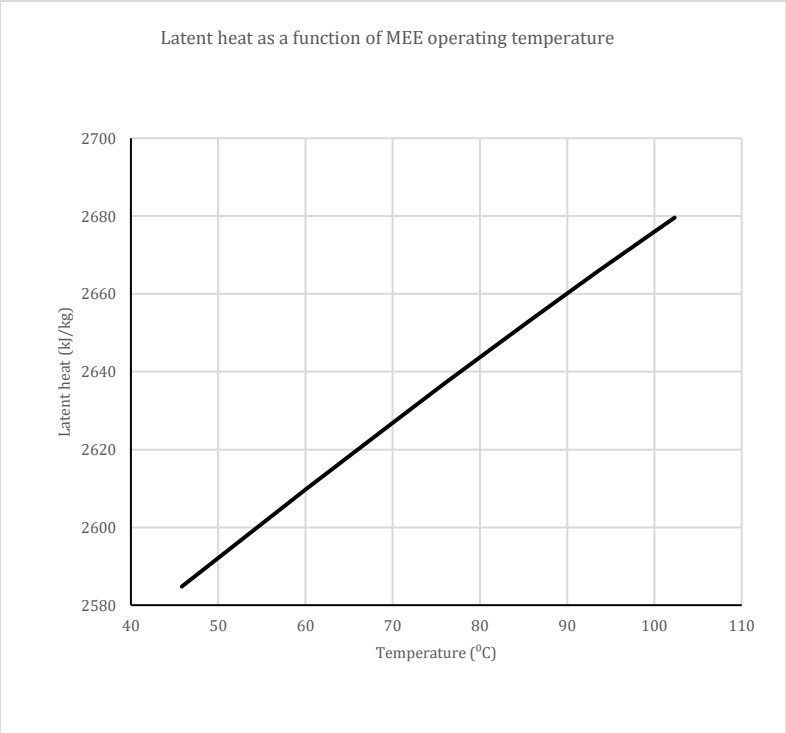

Fig. 3: Plot of latent heat as a function of MEE operating temperature obtained from the steam table (El-Dessouky and Ettouney, 2002)

However, the latent heat depends on the temperature. Therefore, the temperature of each effect must be calculated. The heat load in each evaporator can also be estimated in terms of the evaporator heat transfer area, the temperature driving force, and the overall heat transfer coefficient in each evaporator using the following equation:

$$Q_i = A_i U_i \Delta T_i \quad (8)$$

As the heat transfer areas in each evaporator are equal:

$$\Delta T_i = \frac{U_1 \Delta T_1}{U_i} \quad (9)$$

The overall temperature drop ($\Delta T_t = \sum_1^n \Delta T_i$) in the system is the difference between the steam/storage zone temperature T_s and the last effect's vapor temperature T_n:

$$\Delta T_t = T_s - T_n \quad (10)$$

The temperature in each effect is estimated as:

$$T_1 = T_s - \Delta T_1 \quad (11)$$

$$T_i = T_{i-1} - \frac{U_1 \Delta T_1}{U_i} \text{ for } i > 1 \quad (12)$$

In iterative solutions, the area for heat is needed to verify the validity of the assumptions in the model. This is in addition to the requirement of obtaining these areas to determine their impact on a system's design and performance. The area of the first effect is given by:

$$A_1 = \frac{D_1 \lambda_1}{U_1 (T_s - T_1)} \quad (13)$$

For the other boilers, there is the following correlation for area:

$$A_i = \frac{D_i \lambda_i}{U_i (T_i - \Delta T_{loss})} \quad (14)$$

The drops in temperature due to the thermodynamic losses (ΔT_{loss}) in each evaporator in the system can vary between 0.5 and 3°C (El-Dessouky and Ettouney, 2002). The condenser heat transfer area may be calculated by:

$$A_c = \frac{Q_c}{U_c \frac{(T_f - T_{cw})}{(\ln \frac{T_n - T_{cw}}{T_n - T_f})}} \quad (15)$$

3. Results and discussion

The study showed that drawing feed water from deep wells is the best method for evaporation desalination processes, because, in general, the greater the depth of the well, the higher the water temperature. To demonstrate this relationship, water was taken from different depths and the temperature was measured for the same Mengerian layer. These measurements clearly showed the relationship between the depth of the well and the water temperature. As shown in Fig. 4, at a depth of 1480m, the water temperature was 51°C, and when the depth increased to nearly 1700m, the temperatures were about 58°C, and between those two depths, the temperature increased directly with the depth. However, most of the water in a well is likely to be cooled by the natural mixing of water from different layers inside the well, so the average temperature in the well will be about 55°C.

Even if water is taken from the sea, deep wells can be dug next to the beach to benefit from the heat of the ground, which also means that the water is purer and filtered.

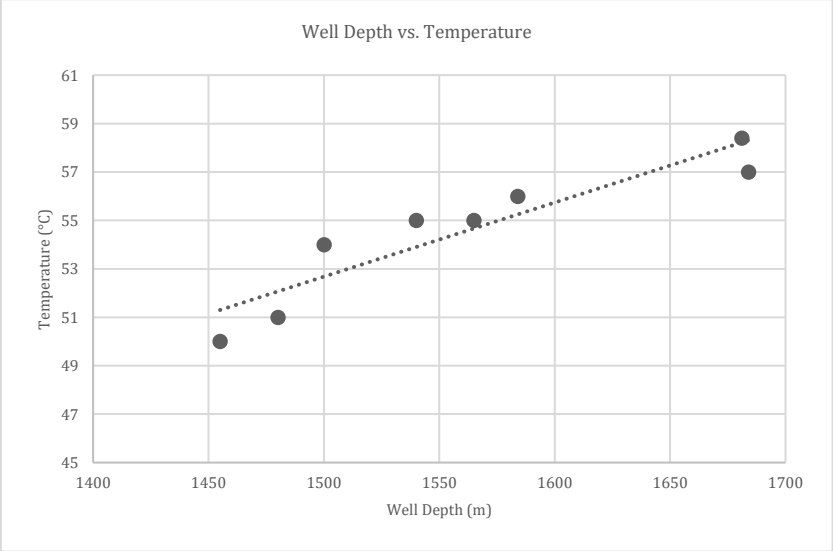

Fig. 4: Relationship between well depth and water temperature

The findings of this study demonstrate that the system performance significantly depends on the first effect's feed-water temperature, which is affected by the storage zone temperature of the salinity pond. The pond heat collection depends on the depth of the gradient layer. To illustrate this relationship, two different GZ (gradient zone) depths, 0.4 and 0.6m, were investigated in this study.

Fig. 5 shows the temperature of the lower region of the salinity gradient pond (SGP) for a non-convecting zone with a depth of 0.4m. It can be seen that at this depth of NCZ, the SGP can operate the MEE plant for 5 summer months in the first year, while during the second year the solar pond can conveniently power the evaporator plant for 7 summer months without any assistance from an external heat source, as during those periods the expected temperature would always be above the threshold of 60°C. Outside those periods the MEE requires an external heat source; for instance, electrical power. The temperatures during the second year of operation are higher due to retained

heat; moreover, even during the first year, the operating temperature can be increased by 2°C by the use of mechanical vapor compressors (MVC).

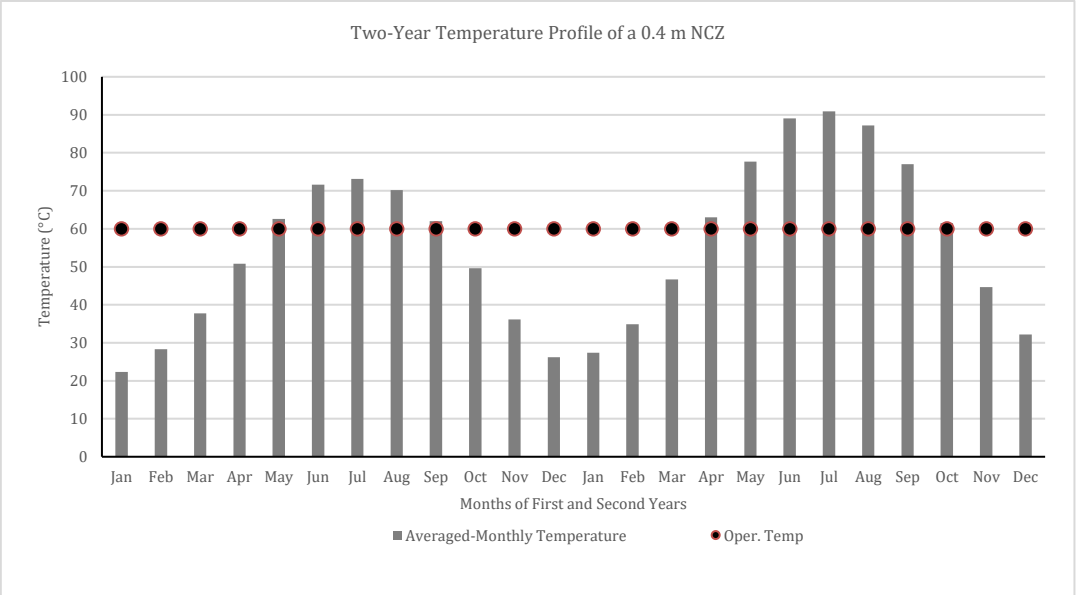

Fig. 5: Temperature changes in a salinity gradient pond with a 0.4m-deep NCZ

The temperature profile of the saline pond for a non-convecting zone whose thickness is increased by 0.2m to 0.6m is plotted in Fig. 6. As expected, the temperatures are higher during the second year of the operation because of the accumulated heat over additional months of solar energy irradiation. This minor increase in the depth of the NCZ may lead to increasing the operating period of the pond from 5 months to 7 summer months in the first year and from 7 months to 9 months in the second year, compared with a middle layer depth of 0.4m. For the other months, the SGP requires only minimal additional heating, as the temperature is not as low as in the case of a 0.4m-deep NCZ. During these operating periods, the expected feed-water temperature may vary from the operating top brine temperature of 60°C to more than 120°C. This poses a potential problem because, during a summer temperature peak in the second year, this maximum storage zone temperature could exceed the boiling temperature of the water. Under such conditions, when boiling occurs, the salinity gradient cannot be maintained in the NCZ. Therefore, heat must be extracted to avoid destroying the pond's salinity structure.

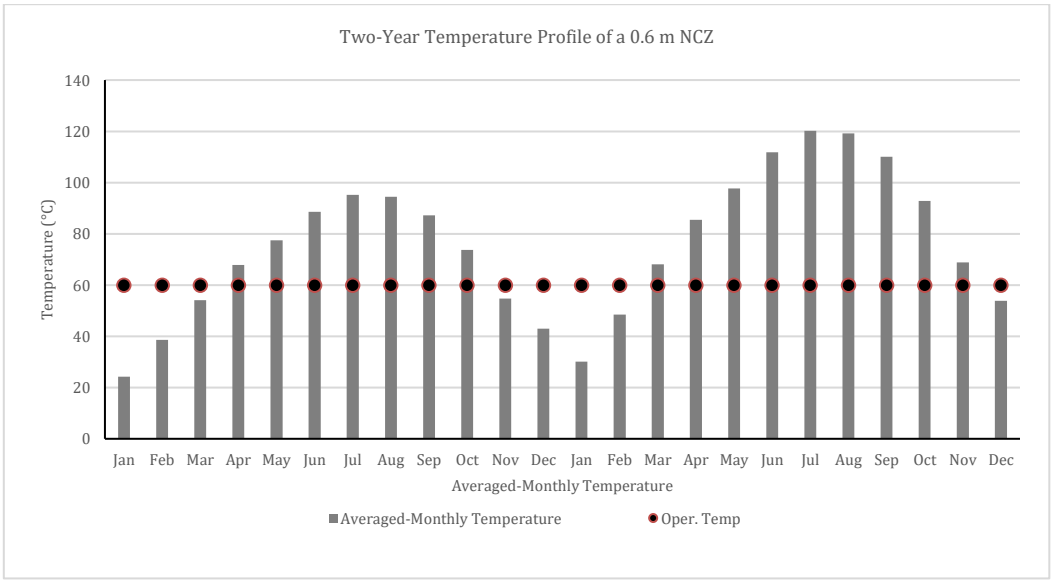

Fig. 6: Temperature of a salinity gradient pond with a 0.6 m-deep NCZ

The required external heat can be supplied by a deep water well, which most villages and small towns in Saudi Arabia rely on. The water temperature in such wells is depth-dependent and could be as high as 50–55°C, and is not significantly affected by seasonal variation, as the wells are deep enough underground to make the influence of weather negligible. Such an approach would reduce the operating costs of the SGP. Using this high intake water temperature, the energy requirements are

significantly lower. The dependence of the multi-effect evaporator plant operation on the well water temperature cannot be neglected and a deeper well should generally provide warmer water. Therefore, the amount of heat required from the solar pond depends greatly on the well water temperature. This relationship has been investigated and the result is plotted in Fig. 7. For deep well water at a relatively high temperature of 55°C, the increase needed to reach the MEE's evaporation temperature is only 5°C, so only 11.2kJ of heat energy is required for each 1kg of water produced. This minimal energy requirement would considerably reduce the operating cost and the water production time.

On the other hand, for an intake of surface water like seawater where the water temperature is lower, a substantially larger amount of heat is needed from the solar pond to reach the desired level: For well or seawater water at 25°C, there is a 35°C deficit to reach the top brine temperature of the first evaporator unit, which represents about 116kJ of heat that must be delivered from the solar pond or another external heat source to desalinate 1kg of raw water

Fig. 7 also shows the big difference in the percentage of dependence on external resources, as the station relies on the solar pond for only 5% of its energy when the inlet water temperature is 55°C, whereas it depends about 88% on external support when the water is drawn from the sea or a shallow well.

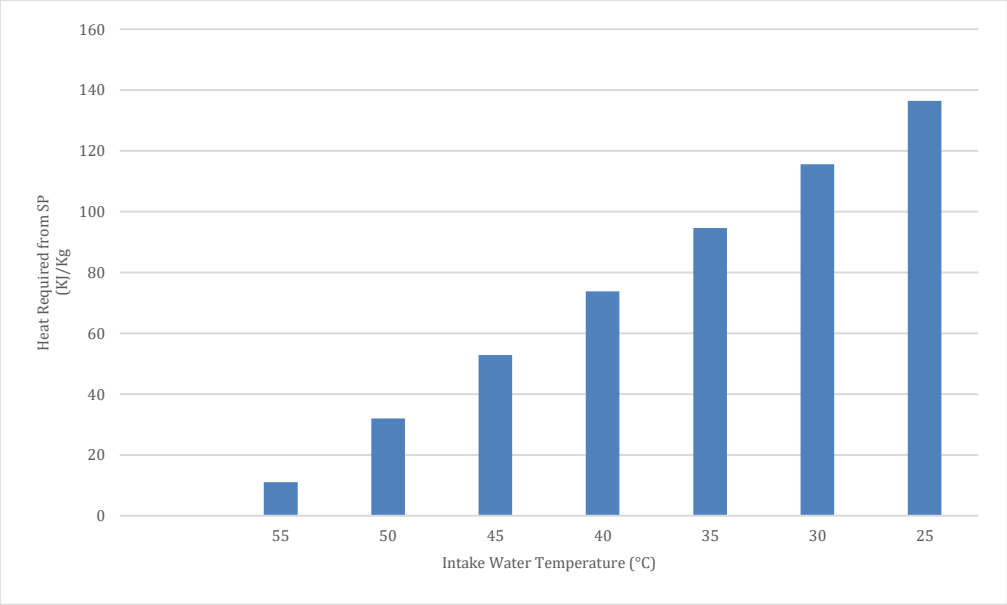

Fig. 7: The heat delivered to the MEE by the solar pond as a function of the water intake temperature

To produce 1m^3/h of freshwater requires ~3.25m^3/h of water flowrate from the solar pond at an operating top brine temperature of 60°C and each effect requires an area of 50.8m^2, while for the same flowrate conditions the required evaporator area is found to be 20m^2 at an operating temperature of 90°C. For a similar evaporator area, the permeate production rate would be increased by almost 3 times and the MEE can be operated from 3–4 evaporators.

4. Conclusion

A multi-effect evaporator, powered by stored solar energy from a salinity gradient solar pond and by geothermal energy from deep wells, is an efficient method of water desalination.

The performance of the system improves with the temperature of the feed-water. Producing 1m^3/h of freshwater requires approximately 3.25m^3/h of water flowrate from the solar pond at an operating top brine temperature of 60°C and each effect requires an area of 50.8m^2.

During the warmer months, this temperature is reached using heat stored in the solar pond. The ability of a salinity gradient solar pond to store heat increases with the depth of its central gradient layer. A pond with an 0.6m central layer can power an MEE for 16 out of its first 24 months without an external heat source.

Most of the shortfalls in the winter months can be supplied by using feed-water from deep wells, because the temperature of well-water increases with increasing depth and does not vary significantly with the seasons. A well whose Mengerian layer is 1500m deep can supply water at approximately 55°C, which is only 5°C short of the MEE's evaporation temperature, so only 11.2kJ of additional heat energy is required for each kilogram of water produced.

This method is well suited to the climate of Saudi Arabia because of the abundance of solar irradiation there. An MEE is efficient and cost-effective, consuming only \$0.06/m^3 in electricity costs, compared with \$0.175/m^3 for a conventional oil-powered thermal plant. This system will therefore save the government money, reduce dependence on

non-renewable fossil fuels, and reduce greenhouse gas emissions.

List of symbols

A	Area (m^2)
A_c	Condenser heat transfer area (m^2)
B	Brine flow rate in i^{th} effect (kg/s)
C_{ps}	Specific heat capacity of the storage zone water (J/kg.°C)
D	Distillate flow rate (kg/s)
D_i	Distillate flow rate in i^{th} effect (kg/s)
F	Feed flow rate (m^3/s)
Q_c	Condenser heat load (W)
Q_i	Thermal load in i^{th} effect (W)
Q_{sb}	Heat lost from the bottom in the storage zone ($W.m^{-2}$)
Q_{se}	Heat lost by heat extraction in the storage zone ($W.m^{-2}$)
Q_{srs}	Heat absorbed from solar radiation in the storage zone ($W.m^{-2}$)
Q_{sru}	Heat absorbed from solar radiation in the upper zone ($W.m^{-2}$)
Q_{st}	Heat lost from the top in the storage zone ($W.m^{-2}$)
Q_{sw}	Heat lost from the sides in the storage zone ($W.m^{-2}$)
S	Water flow rate in the steam/storage zone (kg/s)
T	Temperature (°C)
T_i	Temperature in the i^{th} effect (°C)
T_{cw}	Intake temperature (°C)
T_f	Feed temperature (°C)
T_n	Vapor temperature in the last effect (°C)
T_s	Steam/storage zone temperature (°C)
ΔT_i	Temperature driving force in the i^{th} effect (°C)
ΔT_{loss}	Temperature drop due to thermodynamic losses (°C)
ΔT_t	Overall temperature drop in the system (°C)
U_i	Overall heat transfer coefficient for the i^{th} effect ($W/m^2.°C$)
U_c	Condenser heat transfer coefficient ($W/m^2.°C$)
X_b	Brine concentration (ppmw)
X_i	Brine concentration in the i^{th} effect (ppmw)
X_f	Feed concentration (ppmw)
x_s	Depth of storage zone (m)
λ_i	latent heat formed in i^{th} effect (kJ/kg)
λ_s	latent heat of steam/storage water (kJ/kg)
ρ_s	water density at the storage zone ($kg.m^{-3}$)

Compliance with ethical standards

Conflict of interest

The author(s) declared no potential conflicts of interest with respect to the research, authorship, and/or publication of this article.

References

Al-Shammiri M and Safar M (1999). Multi-effect distillation plants: State of the art. Desalination, 126(1-3): 45-59.

Dickinson W and Cheremisinoff P (1980). Solar energy technology handbook: Part a-engineering fundamentals. Dekker Marcel, New York, USA.

Duffie J and Beckman W (2006). Solar engineering of thermal processes. 3rd Edition, John Wiley and Sons, Hoboken, USA. https://doi.org/10.1016/S0011-9164(99)00154-X

El-Dessouky HT and Ettouney HM (2002). Fundamentals of salt water desalination. Elsevier, New York, USA.

Garmana MA and Muntasserb MA (2008). Sizing and thermal study of salinity gradient solar ponds connecting with the MED desalination unit. Desalination, 222(1-3): 689-695. https://doi.org/10.1016/j.desal.2007.02.074

Geankoplis C (1993). Transport processes and unit operations. 3rd Edition, Prentice-Hall, Hoboken, USA.

Guo Y, Bao M, Gong L, and Shen S (2020). Effects of preheater arrangement on performance of MED desalination system. Desalination, 496: 114702. https://doi.org/10.1016/j.desal.2020.114702

Hongsheng L, Dan W, and MaoZhao X (2020). Experimental study on the thermal performance of a porous medium solar pond. In the 4th International Conference on Green Energy and Applications, IEEE, Singapore, Singapore: 106-110. https://doi.org/10.1109/ICGEA49367.2020.239714

Hull J, Nielsen C, and Golding P (1989). Salinity-gradient solar ponds. CRC Press, Boca Raton, USA. https://doi.org/10.1007/978-1-4613-9945-2_6

Kalogirou SA (2001). Effect of fuel cost on the price of desalination water: A case for renewables. Desalination, 138(1-3): 137-144. https://doi.org/10.1016/S0011-9164(01)00255-7

Kreider J and Kreith F (1981). Solar energy handbook. McGraw-Hill, New York, USA. https://doi.org/10.1115/1.3266267

Lu H, Walton JC, and Swift AH (2001). Desalination coupled with salinity-gradient solar ponds. Desalination, 136(1-3): 13-23. https://doi.org/10.1016/S0011-9164(01)00160-6

Mesa AA, Gómez CM, and Azpitarte RU (1997). Energy saving and desalination of water. Desalination, 108(1-3): 43-50. https://doi.org/10.1016/S0011-9164(97)00007-6

Micale G, Rizzuti L, and Cipollina A (2009). Seawater desalination: conventional and renewable energy processes. Volume 1, Springer, Berlin, Germany. https://doi.org/10.1007/978-3-642-01150-4

NASA (2021). Prediction of worldwide energy resources: The power project. Available online at: https://power.larc.nasa.gov

Ophir A and Lokiec F (2005). Advanced MED process for most economical sea water desalination. Desalination, 182(1-3): 187-198. https://doi.org/10.1016/j.desal.2005.02.026

Porteous A (1983). Desalination technology: Developments and practice. 2nd Edition, Applied Science Publishers, London, UK.

Shahzad MW, Burhan M, Ghaffour N, and Ng KC (2018). A multi evaporator desalination system operated with thermocline energy for future sustainability. Desalination, 435: 268-277. https://doi.org/10.1016/j.desal.2017.04.013

Sharif AO, Al-Hussaini H, and Alenezi IA (2011). New method for predicting the performance of solar pond in any sunny part of the world. In the World Renewable Energy Congress-Sweden, Linköping University Electronic Press, Linköping, Sweden: 3702-3709. https://doi.org/10.3384/ecp110573702

Zell E, Gasim S, Wilcox S, Katamoura S, Stoffel T, Shibli H, and Al Subie M (2015). Assessment of solar radiation resources in Saudi Arabia. Solar Energy, 119: 422-438. https://doi.org/10.1016/j.solener.2015.06.031